

2010

Thermal Analysis of a Small Hermetic Reciprocating Compressor

Serkan Kara

Arcelik A. S.

Emre Oguz

Arcelik A. S.

Follow this and additional works at: <http://docs.lib.purdue.edu/icec>

Kara, Serkan and Oguz, Emre, "Thermal Analysis of a Small Hermetic Reciprocating Compressor" (2010). *International Compressor Engineering Conference*. Paper 1993.

<http://docs.lib.purdue.edu/icec/1993>

This document has been made available through Purdue e-Pubs, a service of the Purdue University Libraries. Please contact epubs@purdue.edu for additional information.

Complete proceedings may be acquired in print and on CD-ROM directly from the Ray W. Herrick Laboratories at <https://engineering.purdue.edu/Herrick/Events/orderlit.html>

Thermal Analysis of a Small Hermetic Reciprocating Compressor

Serkan KARA^{1,*}, Emre OGUZ²

¹Arcelik A.S., Compressor R&D Center
Compressor Plant, Organize Sanayi Bolgesi, 1. Cadde, Eskisehir, Turkey
Phone: +90 222 213 4654, Fax: +90 222 213 4344, serkan.kara@arcelik.com

²Arcelik A.S., R&D Center, 34950 Tuzla
Istanbul, Turkey
Phone: +90 216 585 8019, Fax: +90 216 423 3045, emre.oguz@arcelik.com

* Corresponding Author

ABSTRACT

The mechanical and electric motor efficiencies of new generation hermetic reciprocating compressors for household type refrigerators are relatively higher than the thermodynamic efficiency and very close to their limits under current economical circumstances. Therefore, thermodynamic efficiency is thought to be the main issue for researchers in the near future. This paper presents a thermal analysis of a small hermetic reciprocating compressor focusing on the role of the crankcase on the heating effect of the refrigerant gas along its flow path. The main regions of refrigerant gas flow path in the compressor are associated with the crankcase and some of them such as the compression chamber, crankcase connection bore and the discharge mufflers are actually an integral part of it. The other parts of the flow path like the suction muffler, suction chamber, discharge chamber and the discharge tube are strictly connected to the crankcase. Hence, the crankcase is one of the most important parts in the compressor regarding the heat transfer processes associated with the refrigerant gas. Heat is transferred to the crankcase by conduction, convection and radiation from the nearby thermal sources and these fluxes to the crankcase cause the superheating of the refrigerant gas.

In this study, a commercially available Computational Fluid Dynamics (CFD) code is used to carry out the thermal analysis of the crankcase. Two different configurations are taken into account where some of the boundary conditions are obtained from experimental studies and fundamental heat transfer correlations. This approach is used as a part of the studies to establish a general code for the performance prediction of compressors where the gas temperatures can be calculated via a one-dimensional transient simulation and the crankcase temperature can be obtained with the aid of a commercial solver.

1. INTRODUCTION

In order to decrease the power consumption of the compressor, main issues for R&D engineers are the mechanical efficiency, motor efficiency and the thermodynamic efficiency of the compressor. Mechanical and motor efficiencies are very close to their limits for new generation compact compressors under current economical circumstances but the thermodynamic efficiency level is far away from its limit. Hence, R&D engineers have been hardly working to understand the thermal phenomenon in the compressor and to improve the thermodynamic efficiency of the compressor.

There are many interesting studies in the literature concerning the compressor thermodynamics and heat transfer phenomena. The studies presented by Perez-Segerra *et al.* (2005), Almbauer *et al.* (2006), Abidin *et al.* (2006), Todescat *et al.* (1992) and Birari (2006) applied different numerical methods and experimental techniques to solve the heat transfer mechanisms inside the compressor. It was shown that the heat transfer mechanisms in the compressor had been very complicated and lots of resources had been necessary to perform a study which exactly describes all of the heat transfer processes associated with the gas and oil flow; conduction and radiation and the thermal energy generated due to compression and viscous friction.

Crank case is one of the most important parts effecting the heat transfer mechanisms related to the thermodynamics processes inside the compressors. Almost all of the components in the compressor are either attached to or very close to the crankcase which requires the definition of the heat transfer mechanisms associated with these components. As seen in Figure 1, the crankcase interacts with many components and different heat transfer mechanisms take place between the crankcase and the other parts via conduction, convection and radiation.

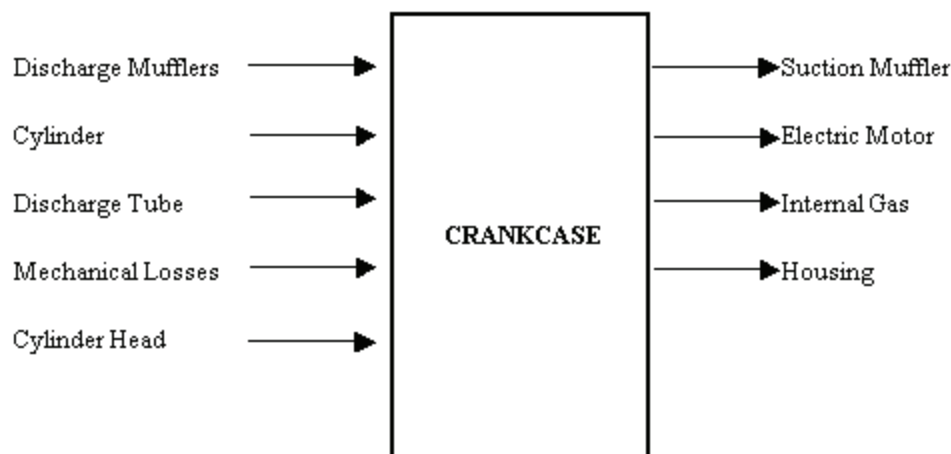


Figure 1. Heat transfer paths associated with the crankcase

As a part of the studies to establish a general code for the performance prediction of compressors where the gas temperatures can be calculated via a one-dimensional transient simulation and the crankcase temperature distribution can be obtained with the aid of a commercial solver, some of the above mentioned interactions are neglected to simplify the first version of the analysis. CFD analysis were carried out on two different crankcase configurations with different boundary conditions in order to understand the effect of some of the mechanisms.

2. EXPERIMENTAL STUDIES

2.1 Instrumentation and Test System

Experimental studies were performed to have the thermal map of the compressor model under investigation. The tested compressor is designed for R600a applications and the cooling capacity at ASHRAE conditions is 200W. The tests were performed on two different configurations: Model A, which has two discharge chambers and Model B which has a single discharge muffler on the crankcase. Both of the models were instrumented with T-type thin thermocouples that were located to different points inside the compressors. The thermocouple locations are given in Table 1.

The temperature measurements were performed while the compressors were running on a fully automated calorimeter system that enabled stabilised operating conditions at ASHRAE point; namely +54.4°C condensation and -23.3°C evaporation temperatures. The subcool, superheat and the ambient temperature for the compressor were all set to 32.2°C. After the calorimeter test is started each test takes about four hours in order to ensure the thermal stabilization of all the components inside the compressor. During the last 60 minutes of the test DAQ system was used to collect the temperature data.

Table 1. Thermocouple locations on the compressors

No	Temperature measurement locations
G1	Cylinder head discharge manifold (Gas)
G2	Connection between discharge manifold and 1 st discharge muffler*
G3	Discharge muffler-1 (Gas)
G4	Discharge muffler-2 (Gas)
G5	Gas inside the shell (Close to the top of the upper shell)
S1	Cylinder Head (Metal)
S2	Connection-1 (Metal, between dis. manifold and 1 st dis. muffler)
S3	Discharge muffler-1 (Metal)
S4	Connection-2 (Between the 1 st and 2 nd dis. mufflers)
S5	Discharge muffler-2 (Metal)
S6	Crankcase rear-1 (First discharge muffler side, metal)
S7	Crankcase rear-2 (Second discharge muffler side, metal)
S8	Crankcase cylinder bore-front (Metal)
S9	Crankcase cylinder bore-rear (Metal)
S10	Upper main winding-2nd discharge muffler side (Metal)
S11	Upper main winding-1st discharge muffler side (Metal)
S12	Lower main winding-1st discharge muffler side (Metal)
S13	Lamination-1st discharge muffler side-mid (Metal)
S14	Upper Housing (Metal)

* This temperature is not actually measured but estimated based on the inlet and outlet temperatures of the associated section.

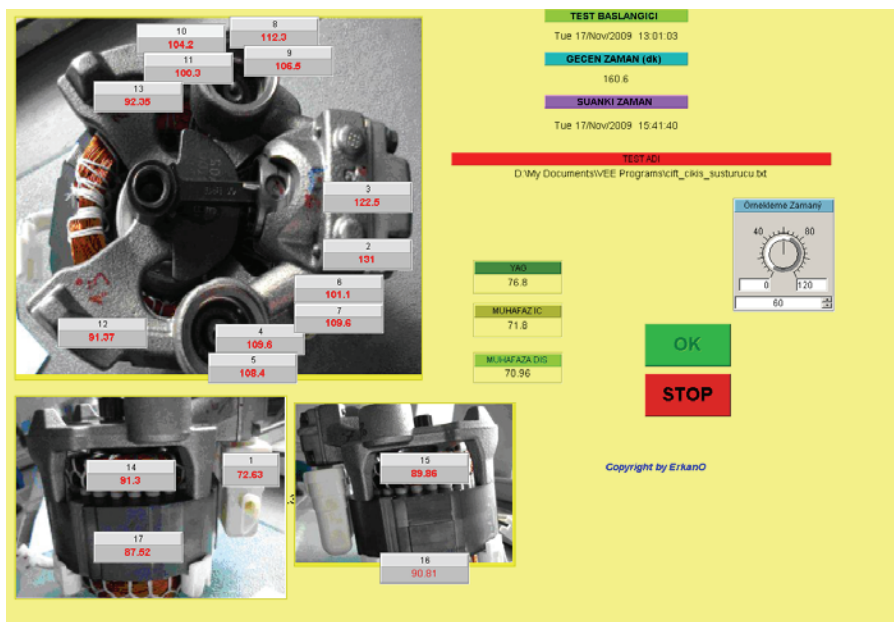


Figure 2. DAQ software interface

2.2 Experimental Results

The results of the temperature measurements performed on both of the compressor models are given in Table 2 for the gas path and in Table 3 for the solid parts. As it can be seen from Table 2, the highest temperature for both of the models appears in the cylinder head where the high pressure high temperature gas is discharged after the compression process. For model A, the temperature of the gas drops to 115.8°C and then to 112.0°C while it flows to the first discharge muffler. As a result of the heat transfer that occurs through the tubing that connects the two mufflers, the temperature further decreases to 103.8°C.

When model A and model B compressor high pressure gas paths are compared, it can be concluded that the temperature of the gas decreases approximately 5K as a result of the elimination of the second discharge muffler. This decrease is thought to be an indirect consequence of this design change since the major difference in the heat transfer network of the two models is the amount of energy transferred from the high temperature gas to the crankcase via the second muffler. This effect becomes more clear when the temperatures of the solid parts given in Table 3 are compared for the two models where the distributions are also graphically represented in Figure 3. When Model A compressor is considered alone, it can be seen that the highest temperature appears on the cylinder head where the high temperature high pressure gas is discharged after the compression process. Since the second discharge muffler is eliminated in Model B, the major difference in temperatures when compared with Model A appears on TC number S5, discharge muffler – 2 location. The elimination of the thermal energy that is originally transferred to the crankcase from the second discharge muffler causes a decrease in all of the temperatures as a result of the change in the thermal balance of the crankcase. In addition to the second discharge muffler, the rear part of the crankcase is also effected and the temperature in this region drops almost 8K. There is an average temperature drop of approximately 5K for all of the other solid parts.

As a result of the experimental studies it can be concluded that there can be a temperature difference up to 30K between the solid parts associated with the crankcase depending on the design of the compressor. It can further be concluded that eliminating one of the thermal inputs to the crankcase may change the gas temperatures in turn by affecting both the cylinder compression process by decreasing the cylinder liner temperature and the general temperature distribution of the crankcase.

Table 2. Experimental temperature distribution of the gas

TC Number	Location	Model A (°C)	Model B (°C)	Difference (K)
G1	Cylinder head (dis.)	131.9	126.9	-5.0
G2	Connection-1	115.8	110.4	-5.4
G3	Discharge muffler-1	112.0	108.0	-4.0
G4	Discharge muffler-2	103.8	N/A	N/A
G5	Gas inside the shell	72.0	70.0	-2.0

Table 3. Experimental temperature distribution on the solid parts

TC Number	Location	Model A (°C)	Model B (°C)	Difference (K)
S1	Cylinder head	122.6	117.6	-5.0
S2	Connection-1	109.9	104.5	-5.4
S3	Discharge muffler-1	106.8	101.3	-5.5
S4	Connection-2	101.7	94.6	-7.1
S5	Discharge muffler-2	100.6	89.0	-11.6
S6	Crankcase rear-1	92.7	87.6	-5.1
S7	Crankcase rear-2	91.7	84.0	-7.7
S8	Cylinder bore-front	109.9	104.3	-5.6
S9	Cylinder bore-rear	108.7	102.9	-5.8

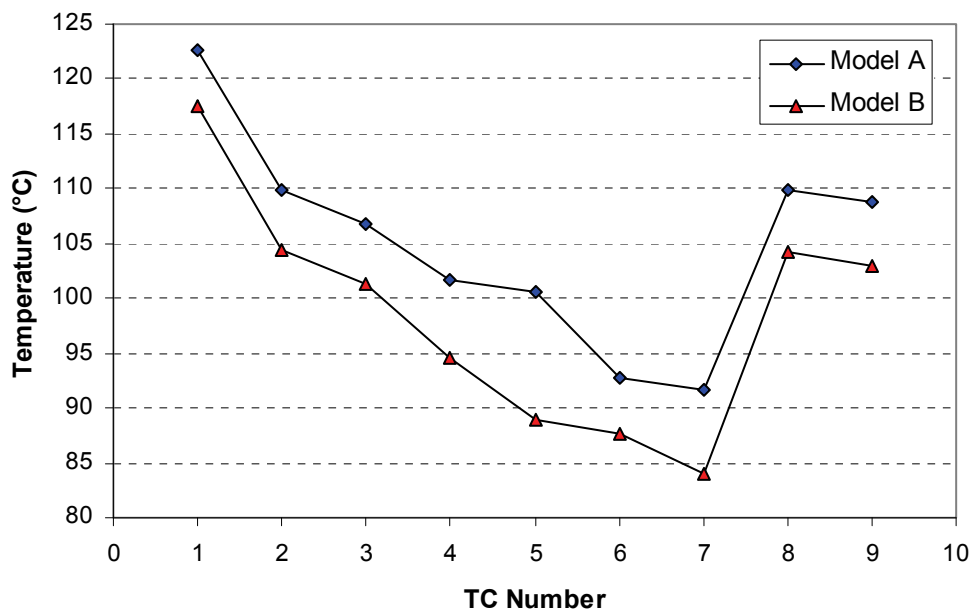


Fig. 3. Experimental temperature distribution on the solid parts

3. NUMERICAL STUDIES

3.1 Numerical Model and Boundary Conditions

A commercially available CFD code (ANSYS FLUENT) was used for the numerical studies. The number of cells for the solution domain is around 250,000. There are three parts in the domain: the crankcase, the valve plate and the cylinder head. Materials for these parts are respectively gray cast iron, steel sheet and aluminium. Gaskets are not modeled among these three parts. The mesh structure of the solution domain is presented in Figure 4.

There are two separate discharge mufflers on the crankcase as it can be seen in Figure 4. One or both of them can be used as discharge mufflers and the simulations were performed for each of the cases. The calculations were performed for steady-state heat transfer.

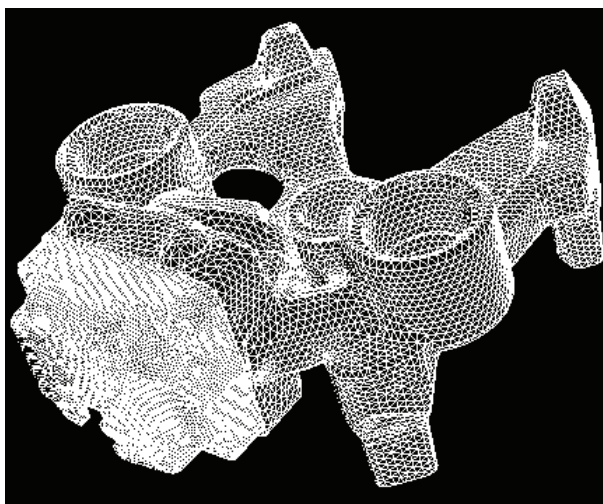


Figure 4. Solution Domain

This solution procedure is supposed to be coupled to a one-dimensional compressor simulation code in the future and therefore some of the temperature boundary conditions are based on the experimental measurements to represent this approach. The heat transfer coefficients for natural and forced convection boundary conditions were based on generally accepted generic values for the associated heat transfer mechanisms (i.e. $25\text{W/m}^2\cdot\text{K}$ for natural and $250\text{W/m}^2\cdot\text{K}$ for forced convection). Other boundary conditions were based on a previous study by Ozdemir (2007). The boundary conditions are summarized in Table 4. In this table q'' , h_n , h_f and T_f are defined as the heat flux, natural convection heat transfer coefficient, forced convection heat transfer coefficient and associated boundary gas temperature. When model A and B boundary conditions are compared, it will be seen that the heat flux for the crankcase crankshaft bore, the cylinder bore and the valve plate cylinder side are set to zero. However, this is not related to the geometrical properties of the models but rather a decision made after the evaluation of the numerical results for model A which will be more clear in the following section. On the other hand, the boundary condition for the 2nd discharge muffler was changed from forced to natural convection when switching from model A to B based on the fact that the second muffler was not used anymore and was exposed to the gas inside the shell.

Table 4. Boundary conditions for the numerical studies

Boundary	Model A	Model B
Crankcase crankshaft bore	q'' : 1800 W/m^2	q'' : 0 W/m^2
2 nd Discharge muffler	h_f : $250\text{ W/m}^2\cdot\text{K}$, T_f : 103.8°C	h_n : $25\text{ W/m}^2\cdot\text{K}$, T_f : 70.0°C
1 st Discharge muffler	h_f : $250\text{ W/m}^2\cdot\text{K}$, T_f : 112.0°C	h_f : $250\text{ W/m}^2\cdot\text{K}$, T_f : 108.0°C
Connection-1 liner	h_f : $250\text{ W/m}^2\cdot\text{K}$, T_f : 115.8°C	h_f : $250\text{ W/m}^2\cdot\text{K}$, T_f : 110.4°C
Crankcase cylinder bore	q'' : 4250 W/m^2	q'' : 0 W/m^2
Cylinder head dis. manifold	h_f : $250\text{ W/m}^2\cdot\text{K}$, T_f : 131.9°C	h_f : $250\text{ W/m}^2\cdot\text{K}$, T_f : 126.9°C
Valve plate cylinder side	q'' : 1000 W/m^2	q'' : 0 W/m^2
Valve plate discharge side	h_f : $250\text{ W/m}^2\cdot\text{K}$, T_f : 131.9°C	h_f : $250\text{ W/m}^2\cdot\text{K}$, T_f : 126.9°C
Gas inside the shell	h_n : $25\text{ W/m}^2\cdot\text{K}$, T_f : 72.0°C	h_n : $25\text{ W/m}^2\cdot\text{K}$, T_f : 70.0°C

3.2 Numerical Results and Discussion

The results of the numerical calculations for model A compressor are given in Figure 5. It has to be remembered that the gas temperatures which were experimentally determined are used as the boundary conditions for these simulations. Therefore, the results are the solution of the conduction heat transfer inside the crankcase rather than a complete CFD solution of the whole compressor control volume. When the experimental values given in Figure 5 are compared with the results of numerical case study # 1, it can be seen that the general distribution inside the crankcase can be calculated to a certain degree of accuracy even though average convective heat transfer coefficients from the literature are applied as boundary conditions where necessary. The major differences in the temperature distribution occurred at location 4 (connection-2), location 8 (cylinder bore front) and 9 (cylinder bore rear) where the differences are on the order of 7 to 9K.

Since the cylinder bore temperatures were over predicted, the heat flux boundary conditions for the cylinder and the valve plate (cylinder facing surface) were set to zero for numerical case # 2 to understand the effect of this heat transfer. When Figure 5 is examined, it can easily be seen that the cylinder bore temperatures match much better with the experimental values (locations 8 and 9). In addition to this, the temperature of location 4 (connection-2) is also now predicted to a good degree of accuracy. However, since the total energy transfer to the crankcase is decreased, a temperature drop of approximately 5K also occurs in locations 1 and 2, cylinder head and connection-1.

A further change in the boundary conditions was applied and the heat flux on the main bearing surface which was representing the viscous loss was set zero in numerical case # 3. This change again effected almost all of the temperatures but mainly the temperatures of locations 6 and 7 (crankcase rear 1 and 2) dropped 3K and except the cylinder head and first discharge muffler all temperatures are well within $\pm 3\text{K}$ when compared with the experimental values.

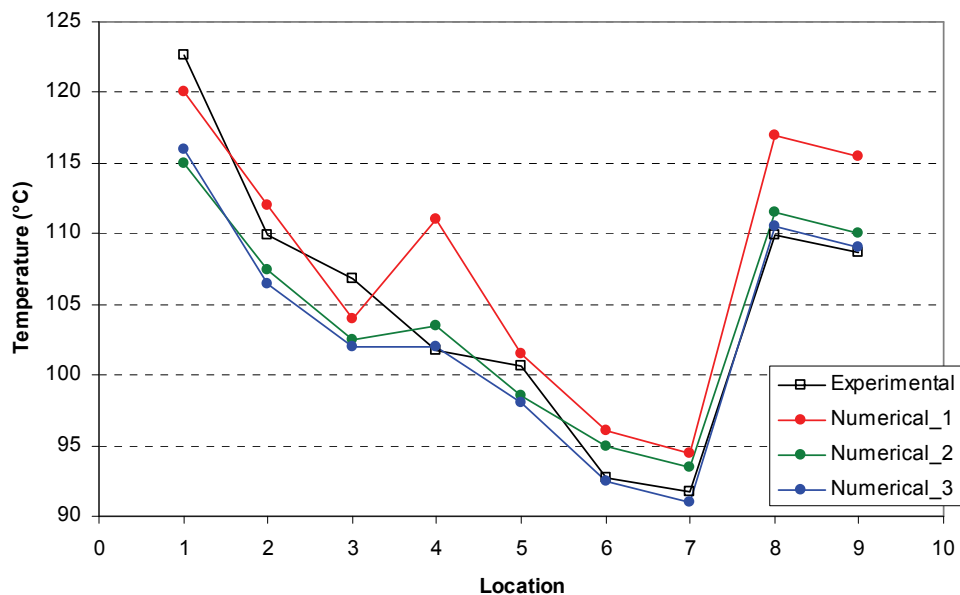


Fig. 5. Experimental temperature distribution on the solid parts, model A

The results of the numerical calculations for model B compressor are given in Figure 6. One important point in these simulations is that, the numerical case # 1 uses the boundary conditions that were applied for model A before in order to understand how well the prediction would be without updating the boundary conditions. This situation represents the solution of a new design when there is no code available to update the gas temperatures. When Figure 6 is examined, it can be argued that the temperature predictions are well within $\pm 5\text{K}$ and the general distribution is very well represented. The numerical case #2 is represented by the boundary conditions already given in Table 4 where the associated gas temperatures are again based on the experimental measurements. Since the second discharge chamber is eliminated and the total energy to the crankcase is decreased, this in turn affects the temperature of the gas through its flow path as discussed before. This change in temperature definitely effects the temperature distribution of the crankcase as shown in Figure 6. Most of the temperatures including the crankcase rear and cylinder bore are well within $\pm 2\text{K}$ when compared with the experimental values given in Table 3.

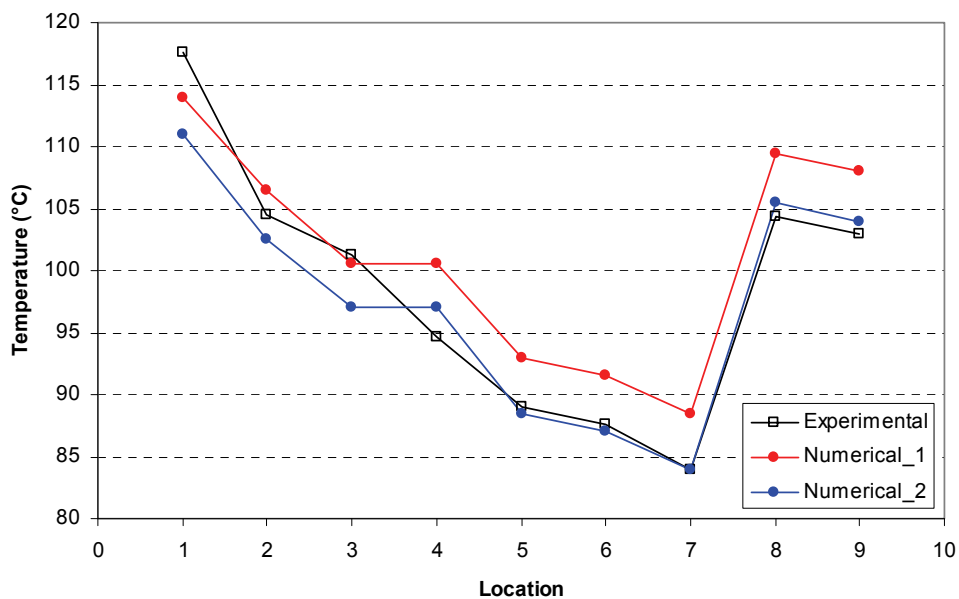


Fig. 6. Experimental temperature distribution on the solid parts, model B

4. CONCLUSIONS

In this study, the temperature distribution of two different crankcase designs were investigated both experimentally and numerically. Temperature measurements were performed to obtain the gas and solid temperatures and the numerical simulations were based on the measured gas temperatures with additional convective heat transfer boundary conditions based on the generally accepted generic values in the literature. The effect of the boundary conditions were examined and a first step for a procedure to couple one-dimensional compressor simulation codes with 3D numerical solutions was established. Based on the results of this study it can be concluded that:

- There can be a temperature gradient up to 30K between the solid components directly attached to the crankcase and the crankcase itself depending on the specific design of the compressor. This distribution is closely related to the existence and number of discharge mufflers.
- When one of the two mufflers widely used in today's designs is eliminated, the thermal energy input to the crankcase is decreased which in turn effects and decreases the temperature of the high pressure gas up to 7K. Therefore a simulation procedure where the crankcase is represented as a single thermal component will not be sufficient to accurately calculate the effects of design changes.
- Although generic values for various convective heat transfer coefficients are used relatively good agreement has been observed between the numerical and experimental temperature values. However it is still not clear how much the temperatures will be effected when exactly determined convective heat transfer coefficients are used which requires important numerical efforts (pulsating nature of the flow and non-standard geometry of the components etc.)
- In this study the temperature of the gas inside the shell is assumed to be constant, however experimental studies show that there might exist a variation up to 15K. Therefore dividing the gas volume into smaller components which are in interaction with different components might increase the accuracy of such calculations.

REFERENCES

- Abidin, Z., *et al.*, 2006, Domain Decomposition Method for 3-Dimensional Simulation of the Piston Cylinder Section of a Hermetic Reciprocating Compressor *Proc. Int. Compressor Engineering Conference at Purdue*, Purdue University, West Lafayette, USA
- Almbauer, R.A., *et al.*, 2006, 3-Dimensional Simulation for Obtaining the Heat Transfer Correlations of a Thermal Network Calculation for a Hermetic Reciprocating Compressor, *Proc. Int. Compressor Engineering Conference at Purdue*, Purdue University, West Lafayette, USA
- Birari, Y.V., *et al.*, 2006, Use of CFD in Design and Development of R404a Reciprocating Compressor, *Proc. Int. Compressor Engineering Conference at Purdue*, Purdue University, West Lafayette, USA
- Ozdemir, A.R., 2007, *An Investigation of the Heat Transfer Characteristics Among the Hermetic Reciprocating Compressor Components*, M.Sc. Thesis, Istanbul Technical University, Istanbul, Turkey
- Perez-Segarra, C.D. *et al.*, 2005, Detailed Thermodynamic Characterization of Hermetic Reciprocating Compressors, *International Journal of Refrigeration*, Volume 28, Issue 4: Pages 459-631
- Todescat, M.L., *et al.*, 1992, Thermal Energy Analysis in Reciprocating Hermetic Compressors, *Proc. Int. Compressor Engineering Conference at Purdue*, Purdue University, West Lafayette, USA